Submitted to

33rd International Conference on High Energy Physics, ICHEP06, July. 26-Aug.2, 2006, Moscow

Abstract: **7-0004**

Parallel Session **7**

www-h1.desy.de/h1/www/publications/conf/conf_list.html

Charged current interactions in ep scattering at HERA with longitudinally polarised electrons

H1 Collaboration

Abstract

Data taken with electrons of different longitudinal polarisation states in collision with unpolarised protons at HERA are used to measure the total cross sections of the charged current process, $e^-p \to \nu X$, for negative four-momentum transfer squared $Q^2 > 400\,\mathrm{GeV}^2$ and inelasticity $y < 0.9$. Together with the corresponding cross section obtained from the previously published unpolarised data, the polarisation dependence of the charged current cross section is measured and found to be in agreement with the Standard Model prediction. The e^-p data and the recently published e^+p data are also used to measure the single differential cross sections $\mathrm{d}\sigma/\mathrm{d}Q^2$.

1 Introduction

The ep collider HERA has been running in the second phase (HERA-II) since autumn 2003 with a longitudinally polarised positron or electron beam. The first e^+p data collected by the H1 and ZEUS experiments have been published recently [1, 2]. The e^-p data are being taken and part of the data has been analysed with the preliminary results reported [3].

Measurements of deep inelastic scattering (DIS) with polarised leptons on protons allow the parton distribution functions (PDFs) of the proton to be further constrained through polarisation asymmetries [4] and specific tests of the electroweak (EW) parts of the Standard Model to be performed [5, 6]. In particular, the measurements presented here extend the tests of the $\mathrm{V}-\mathrm{A}$ structure of charged current interactions from low Q^2 [7] into the high Q^2 regime, where Q^2 is the negative four-momentum transfer squared.

At HERA DIS proceeding via charged currents (CC), $ep \to \nu X$, and neutral currents (NC), $ep \to eX$, can be measured accurately [8, 9]. The polarisation dependence of the CC and NC cross sections is fixed within the Standard Model framework. Specifically, the Standard Model predicts, from the absence of right handed charged currents, that the CC e^-p cross section is directly proportional to the fraction of left handed electrons in the beam.

In this paper first measurements of the charged current total cross sections, $\sigma_{\mathrm{CC}}^{\mathrm{tot}}$, are reported for two values of longitudinal polarisation, $P_e = (N_R - N_L)/(N_R + N_L)$, with N_R (N_L) being the number of right (left) handed electrons in the beam. The corresponding data sets are termed the R and L data sets respectively. The R data set has a luminosity weighted mean polarisation value of $(37.0\pm1.8)\,\%$ and an integrated luminosity value of $29.6\pm0.6\,\mathrm{pb}^{-1}$. The corresponding numbers for the L data set are $(-27.0\pm1.3)\,\%$ and $68.6\pm1.4\,\mathrm{pb}^{-1}$. In both data sets the incident electron beam energy is $27.5\,\mathrm{GeV}$, whilst the unpolarised proton beam energy is $920\,\mathrm{GeV}$. This yields a centre-of-mass energy of $\sqrt{s} = 318\,\mathrm{GeV}$.

The measurements presented here, as well as the corresponding one obtained using the published unpolarised data, are compared to Standard Model expectations and a linear fit to $\sigma_{\mathrm{CC}}^{\mathrm{tot}}$ as a function of P_e is performed. The result of the fit is used to derive a cross section for a fully right handed electron beam corresponding to $P_e = 1$.

2 Charged Current Cross Section

The measured double differential CC cross section for collisions of polarised electrons with unpolarised protons, corrected for QED radiative effects, may be expressed as

$$\frac{\mathrm{d}^2\sigma_{\mathrm{CC}}}{\mathrm{d}x\mathrm{d}Q^2} = (1-P_e)\frac{G_F^2}{4\pi x}\left[\frac{M_W^2}{M_W^2+Q^2}\right]^2 \left(Y_+W_2 - Y_-xW_3 - y^2W_L\right)\cdot(1+\delta_{\mathrm{weak}}^{\mathrm{CC}})\,, \qquad (1)$$

where x is the Bjorken x variable and y characterises the inelasticity of the interaction. The Fermi constant G_F is defined [10] using the weak boson masses. Other quantities in Eq.(1) include M_W, the mass of the W boson, W_2, xW_3 and W_L, CC structure functions, and $\delta_{\mathrm{weak}}^{\mathrm{CC}}$, the weak radiative corrections. The helicity dependences of the weak interaction are contained in $Y_\pm = 1 \pm (1-y)^2$. In the quark parton model (QPM), where $W_L \equiv 0$, the structure functions W_2 and xW_3 for e^+p scattering may be expressed as the sum and difference of the quark and anti-quark momentum distributions, $xq(x, Q^2)$ and $x\overline{q}(x, Q^2)$:

$$W_2 = x(u + c + \overline{d} + \overline{s})\,, \tag{2}$$
$$xW_3 = x(u + c - \overline{d} - \overline{s})\,. \tag{3}$$

The total cross section, $\sigma_{\mathrm{CC}}^{\mathrm{tot}}$, is defined as the integrated cross section in the kinematic region $Q^2 > 400\,\mathrm{GeV}^2$ and $y < 0.9$. From Eq.(1) it can be seen that the cross section has a linear dependence on the polarisation of the electron beam P_e. For a fully right handed electron beam, $P_e = 1$, the cross section is identically zero in the Standard Model.

3 Experimental Technique

At HERA transverse polarisation of the lepton beam arises naturally through synchrotron radiation via the Sokolov-Ternov effect [11]. In 2000 a pair of spin rotators was installed in the beamline on either side of the H1 detector, allowing transversely polarised leptons to be rotated into longitudinally polarised states and back again. The degree of polarisation is constant around the HERA ring and is continuously measured using two independent polarimeters LPOL [12] and TPOL [13]. The polarimeters are situated in beamline sections in which the beam leptons have longitudinal and transverse polarisations respectively. Both measurements rely on an asymmetry in the energy spectrum of left and right handed circularly polarised photons undergoing Compton scattering with the lepton beam. The TPOL measurement uses in addition a spatial asymmetry. The LPOL polarimeter measurements are used when available and TPOL measurements otherwise. The polarisation profile weighted by the luminosity values is shown in Fig. 1.

The H1 detector components most relevant to this analysis are the liquid argon (LAr) calorimeter, which measures the positions and energies of charged and neutral particles over the polar[1] angular range $4^\circ < \theta < 154^\circ$, and the inner tracking detectors, which measure the angles and momenta of charged particles over the range $7^\circ < \theta < 165^\circ$. A full description of the detector can be found in [14].

Simulated DIS events are used in order to determine acceptance corrections. DIS processes are generated using the DJANGO [15] Monte Carlo (MC) simulation program, which is based on LEPTO [16] for the hard interaction and HERACLES [17] for single photon emission and virtual EW corrections. LEPTO combines $\mathcal{O}(\alpha_s)$ matrix elements with higher order QCD effects using the colour dipole model as implemented in ARIADNE [18]. The JETSET program [19] is used to simulate the hadronisation process. In the event generation the DIS cross section is calculated using the H1 PDF 2000 [8] parametrisation for the proton PDFs.

The dominant ep background contribution arises from photoproduction processes. These are simulated using the PYTHIA [20] MC with leading order PDFs for the proton taken from CTEQ [21] and for the photon from GRV [22]. Further backgrounds from NC DIS, QED-Compton scattering, lepton pair production, prompt photon production and heavy gauge boson

[1]The polar angle θ is defined with respect to the positive z axis, the direction of the incident proton beam.

($W^{\pm}, Z^0$) production are also simulated; their final contribution to the analysis sample is small. Further details are given in [8].

The detector response to events produced by the generation programs is simulated in detail using a program based on GEANT [23]. These simulated events are then subjected to the same reconstruction and analysis chain as the data.

The selection of CC interactions follows closely that of the previously published analysis of unpolarised data from H1 [8] and is briefly described below. The CC events are characterised as having large unbalanced transverse momentum, $P_{T,h}$, attributed to the undetected neutrino. The quantity $P_{T,h}$ is determined from $P_{T,h} = \sqrt{(\sum_i p_{x,i})^2 + (\sum_i p_{y,i})^2}$, where the summation is performed over all particles of the hadronic final state. The hadronic final state particles are reconstructed using a combination of tracks and calorimeter deposits in an energy flow algorithm that avoids double counting [24].

The CC kinematic quantities are determined from the hadonic final state [25] using the relations

$$y_h = \frac{E_h - p_{z,h}}{2\,E_e}\,, \qquad Q_h^2 = \frac{P_{T,h}^2}{1 - y_h}\,, \qquad x_h = \frac{Q_h^2}{s\,y_h}\,, \tag{4}$$

where $E_h - p_{z,h} \equiv \sum_i (E_i - p_{z,i})$ and E_e is the incident electron beam energy.

NC interactions are also studied as they provide an accurate and high statistics data sample with which to check the detector response. The selection of NC interactions is based mainly on the requirement of an identified scattered electron in the LAr calorimeter, with an energy $E'_e > 11\,\mathrm{GeV}$. The NC sample is used to carry out an *in-situ* calibration of the electromagnetic and hadronic energy scales of the LAr calorimeter using the method described in [8, 24, 26, 27]. The hadronic calibration procedure is based on the balance of the transverse energy of the electrons with that of the hadronic final state. The calibration procedure gives good agreement between data and simulation within an estimated uncertainty of 2% on the hadronic scale.

In addition, NC events are used for studies of systematic uncertainties in the charged current analysis. The data are processed such that all information from the scattered electron is suppressed, providing the so-called *pseudo-CC* sample [24, 26, 27]. This sample mimics CC interactions allowing trigger and selection efficiencies to be checked with high statistical precision and independently of the MC simulation.

4 Measurement Procedure

Candidate CC interactions are selected by requiring $P_{T,h} > 12\,\mathrm{GeV}$ and a reconstructed vertex within $35\,\mathrm{cm}$ in z of the nominal interaction point. In order to ensure high efficiency of the trigger and good kinematic resolution the analysis is further restricted to the domain of $0.03 < y_h < 0.85$. The ep background is dominantly due to photoproduction events, in which the scattered electron escapes undetected in the backward direction and transverse momentum is missing due to fluctuations in the detector response or undetected particles. This background is suppressed exploiting the correlation between $P_{T,h}$ and the ratio V_{ap}/V_p of transverse energy flow anti-parallel and parallel to the hadronic final state transverse momentum vector [24, 26, 27]. The suppression cuts are different for the R and L data sets as the relative photoproduction contributions differ in the two samples. The residual ep background is negligible for most of the measured kinematic domain. The simulation is used to estimate this contribution, which is subtracted statistically from the CC data sample. Non-ep background is rejected by searching for typical cosmic ray and beam-induced background event topologies [24, 26, 27]. The final R (L) CC data sample amounts to $\simeq 750$ ($\simeq 3500$) events.

The Q_h^2, $P_{T,h}$, $E_h - p_{z,h}$ and x_h distributions of the selected events are shown in Fig. 2 for the L (upper) and R (lower) samples. The simulation provides a good description of the data. The contribution of background photoproduction processes is small and has the largest influence at low $P_{T,h}$.

Events with $Q_h^2 > 400\,\mathrm{GeV}^2$ are used to measure the cross sections, which correspond to the kinematic region $Q^2 > 400\,\mathrm{GeV}^2$ and $y < 0.9$ and thus are corrected for the effects of the analysis cuts. The correction factor is calculated to be 1.07 using the H1 PDF 2000 parametrisation.

The systematic uncertainties on the cross section measurements are discussed briefly below (see [24, 26, 27] and references therein for more details). Positive and negative variations of one standard deviation of each error source are found to yield errors which are symmetric to a good approximation. The systematic uncertainties of each source are taken to be fully correlated between the cross section measurements unless stated otherwise.

- An uncertainty of 2% is assigned to the scale of the hadronic energy measured in the LAr calorimeter, of which 1% is considered as a correlated component to the uncertainty. This results in a total uncertainty of 1.3% on the cross section measurements.
- A 10% uncertainty is assigned to the amount of energy in the LAr calorimeter attributed to noise, which gives rise to a systematic error of 0.3% on the cross section measurements.
- The variation of cuts against photoproduction on V_{ap}/V_p and $P_{T,h}$ has an effect on the cross sections of 0.6%.
- A 30% uncertainty on the subtracted ep background is determined from a comparison of data and simulation after relaxing the anti-photoproduction cuts, such that the sample is dominated by photoproduction events. This results in a systematic error of 0.5% (1%) on the cross section of the R (L) data.
- The non-ep background finders introduce an inefficiency for CC events. The associated uncertainty is estimated using pseudo-CC data and found to depend on y. An uncertainty of 3% is applied for $y < 0.1$ and 2% for $y > 0.1$. This yields an uncertainty of 2% on the cross section measurements.
- A y-dependent error is assigned to the vertex finding efficiency: 15% for $y < 0.06$, 7% for $0.06 < y < 0.1$, 4% for $0.1 < y < 0.2$ and 1% for $y > 0.2$. This efficiency is estimated using pseudo-CC data yielding an uncertainty of 2.4% on the cross section measurements.
- An uncertainty of 0.5% accounts for the dependence of the acceptance correction on the PDFs used in the MC simulation.

- A 1.8% uncertainty on the trigger efficiency is determined based on the pseudo-CC data sample. The uncorrelated component of this uncertainty is 1%.
- An error of 0.8% is estimated for the QED radiative corrections. This accounts for missing contributions in the simulation of the lowest order QED effects and for the uncertainty on the higher order QED and EW corrections.
- In addition, there is a global uncertainty of 2% on the luminosity measurement for both the R and L data samples, of which 0.5% is considered as correlated.

The total systematic error is formed by adding the individual uncertainties in quadrature and amounts to about 4.4% on the cross section measurements.

The polarisation measurements have a relative uncertainty of 3.5% for the TPOL [28] and 1.6% for the LPOL [12] polarimeter. Some difference between two measurements is observed and is under further investigation. A conservative uncertainty of 5% is quoted for the moment yielding an absolute uncertainty on the mean polarisation of $\pm 1.8\,\%$ for the R sample and $\pm 1.3\,\%$ for the L sample. These are not included in the total systematic error on the cross section measurements, but are considered as independent uncertainties in a linear fit to the data.

5 Results

The measured integrated CC cross sections are quoted in the range $Q^2 > 400\,\mathrm{GeV}^2$ and $y < 0.9$ and are given in Table 1 and shown in Fig. 3. The measurement of the unpolarised total cross section in the same phase space based on $16.4\,\mathrm{pb}^{-1}$ of data collected in 1998 and 1999 is also given. This measurement follows identically the procedure described in [29] but with the Q^2 cut adopted in this analysis. The systematic uncertainties of this unpolarised measurement are taken to be the same as in [8], with the exception of the QED radiative correction uncertainty, which has been reduced from 3% to 0.8%. The measurements are compared to expectations of the Standard Model using the H1 PDF 2000 parametrisation. The uncertainty on the Standard Model expectations combines the uncertainties from experimental data used in the H1 PDF 2000 fit as well as model uncertainties [8].

P_e (%)	$\sigma_{\mathrm{CC}}^{\mathrm{tot}}$ (pb)	SM expectation (pb)
+37.0	$34.5 \pm 1.4_{\mathrm{stat}} \pm 1.5_{\mathrm{sys}}$	35.7 ± 0.4
0.0	$57.0 \pm 2.2_{\mathrm{stat}} \pm 1.4_{\mathrm{sys}}$	56.7 ± 0.6
−27.0	$70.4 \pm 1.2_{\mathrm{stat}} \pm 3.1_{\mathrm{sys}}$	72.0 ± 0.8

Table 1: *Measured cross section values for $\sigma_{\mathrm{CC}}^{\mathrm{tot}}(e^- p \to \nu X)$ in the region $Q^2 > 400\,\mathrm{GeV}^2$ and $y < 0.9$ compared to the Standard Model (SM) expectation.*

A linear fit to the polarisation dependence of the measured cross sections is performed taking into account the correlated systematic uncertainties between the measurements and is shown in Fig. 3. The fit provides a reasonable description of the data with a $\chi^2 = 0.8$ for one degree of freedom. The result of the fit extrapolated to the point $P_e = 1$ yields a fully right handed charged current cross section of

$$\sigma_{CC}^{tot}(P_e = 1) = -0.9 \pm 2.9_{\rm stat} \pm 1.9_{\rm sys} \pm 2.9_{\rm pol}\ \mathrm{pb}\,, \quad (5)$$

where the quoted errors correspond to the statistical (stat), experimental (sys) and polarisation-related (pol) systematic uncertainties. This extrapolated cross section is consistent with the Standard Model prediction of a vanishing cross section and corresponds to an upper limit on $\sigma_{CC}^{tot}(P_e = 1)$ of $8.0\,\mathrm{pb}$ at 95% confidence level (CL), as derived according to [30]. This result excludes the existence of charged currents involving right handed fermions mediated by a boson of mass below $186\,\mathrm{GeV}$ at 95% CL, assuming Standard Model couplings and a massless right handed ν_e.

The L and R data sets have also been combined to obtain a differential cross section measurement $\mathrm{d}\sigma/\mathrm{d}Q^2$. The cross sections shown in Fig. 4 have been corrected for a small residual polarisation effect in the combined data and thus correspond effectively to an unpolarised e^-p data. A similar cross section measurement using the recently published e^+p data has also been obtained and shown in Fig. 4. The behaviour of the CC cross sections at low Q^2 is mainly due to the propagator effect of the massive W boson ($\sim [M_W^2/(Q^2 + M_W^2)]^2$) whereas the difference of CC cross sections between e^-p ad e^+p collisions arises from the difference between the up and down quark distributions and the less favourable helicity factor in the e^+p cross section. The measurements are in good agreement with the corresponding Standard Model expectations determined from the H1 PDF 2000 fit.

6 Summary

The first measurement has been performed of polarised e^-p total charged current cross sections in the kinematic region of $Q^2 > 400\,\mathrm{GeV}^2$ and $y < 0.9$. The results presented here are based on data collected from collisions of unpolarised protons with unpolarised electrons and, for the first time, with longitudinal polarised electrons in left and right helicity states. The polarisation dependence of the charged current cross section has thus been established at HERA both in e^+p and in e^-p collisions, extending previous tests of the chiral structure of the charged current interaction into the region of large, space-like Q^2. The data are found to be consistent with the Standard Model axiomatic absence of right handed charged currents.

The e^-p data and the recently published e^+p data have been further used to obtain the Q^2 dependence of the charged current cross sections. The e^-p data in particular represent a six-fold increase in statistics in comparison with the unpolarised data available at HERA-I.

Acknowledgements

We are grateful to the HERA machine group whose outstanding efforts have made this experiment possible. We thank the engineers and technicians for their work in constructing and maintaining the H1 detector, our funding agencies for financial support, the DESY technical staff for continual assistance and the DESY directorate for support and for the hospitality which they extend to the non DESY members of the collaboration.

References

[1] A. Aktas *et al.* [H1 Collaboration], Phys. Lett. B **634** (2006) 173 [hep-ex/0512060].

[2] S. Chekanov *et al.* [ZEUS Collaboration], hep-ex/0602026.

[3] B. Antunovic, "Charged current in polarised $e^{\pm}p$ collisions at HERA-II", presented at DIS 2006 on behalf of the H1 Collaboration.

[4] M. Klein and T. Riemann, Z. Phys. C **24** (1984) 151.

[5] A. Aktas *et al.* [H1 Collaboration], Phys. Lett. B **632** (2006) 35 [hep-ex/0507080].

[6] R. Beyer *et al.*, Proceedings of the Workshop "Future Physics at HERA", vol. 1, eds. W. Buchmüller, G. Ingelman, A. De Roeck and R. Klanner, DESY (1996) 142;
R. Cashmore *et al.*, ibid., 163.

[7] M. Jonker *et al.* [CHARM Collaboration], Phys. Lett. B **86** (1979) 229.

[8] C. Adloff *et al.* [H1 Collaboration], Eur. Phys. J. C **30** (2003) 1 [hep-ex/0304003].

[9] C. Adloff *et al.* [H1 Collaboration], Eur. Phys. J. C **21** (2001) 33 [hep-ex/0012053].

[10] A. Arbuzov, D.Y. Bardin, J. Bluemlein, L. Kalinovskaya and T. Riemann, Comput. Phys. Commun. **94**, 128 (1996) [hep-ph/9511434].

[11] A.A. Sokolov and I.M. Ternov, Sov. Phys. Dokl. **8** No. 12 (1964) 1203.

[12] M. Beckmann *et al.*, Nucl. Instrum. Meth. A **479** (2002) 334.

[13] D.P. Barber *et al.*, Nucl. Instrum. Meth. A **329** (1993) 79.

[14] I. Abt *et al.* [H1 Collaboration], Nucl. Instrum. Meth. A **386** (1997) 310 and 348;
R.D. Appuhn *et al.* [H1 SPACAL Group], Nucl. Instrum. Meth. A **386** (1997) 397.

[15] G.A. Schuler and H. Spiesberger, Proceedings of the Workshop "Physics at HERA", vol. 3, eds. W. Buchmüller, G. Ingelman, DESY (1992) 1419.

[16] G. Ingelman, Proceedings of the Workshop "Physics at HERA", vol. 3, eds. W. Buchmüller, G. Ingelman, DESY (1992) 1366.

[17] A. Kwiatkowski, H. Spiesberger and H.-J. Möhring, Comput. Phys. Commun. **69** (1992) 155.

[18] L. Lönnblad, Comput. Phys. Commun. **71** (1992) 15.

[19] T. Sjöstrand and M. Bengtsson, Comput. Phys. Commun. **43** (1987) 367.

[20] T. Sjöstrand, Comput. Phys. Commun. **82** (1994) 74.

[21] H.L. Lai *et al.* [CTEQ Collaboration], Eur. Phys. J. C **12** (2000) 375 [hep-ph/9903282].

[22] M. Glück, E. Reya and A. Vogt, Phys. Rev. D **46** (1992) 1973.

[23] R. Brun *et al.*, GEANT3 User's Guide, CERN-DD/EE-84-1 (1987).

[24] B. Portheault, Ph.D. thesis (March 2005), LAL 05-05 (IN2P3/CNRS), Université de Paris-Sud XI, Orsay, available at http://www-h1.desy.de/publications/theses_list.html.

[25] A. Blondel and F. Jacquet, Proceedings of the Study of an ep Facility for Europe, ed. U. Amaldi, DESY (1979) 391.

[26] A. Aktas, Ph.D. thesis (August 2005), Hamburg University, available at http://www-h1.desy.de/publications/theses_list.html.

[27] R. Plačakytė, Ph.D. thesis (*in preparation)*, Max-Planck-Institut für Physik, Munich, will be available at http://www-h1.desy.de/publications/theses_list.html.

[28] W. Lorenzon [HERMES Collaboration], DESY-HERMES-97-68, *7th International Workshop on Polarized Gas Targets and Polarized Beams*, Urbana, IL, 18-22 Aug 1997;
F. Corriveau *et al.* [TPOL Polarimeter Group], "A Calibration of the HERA Transverse Polarimeter for the 2003/2004 Data", available at http://www.desy.de/∼pol2000/documents/documents.html.

[29] C. Adloff *et al.* [H1 Collaboration], Eur. Phys. J. C **19** (2001) 269 [hep-ex/0012052].

[30] G.J. Feldman and R.D. Cousins, Phys. Rev. D **57** (1998) 3873 [physics/9711021].

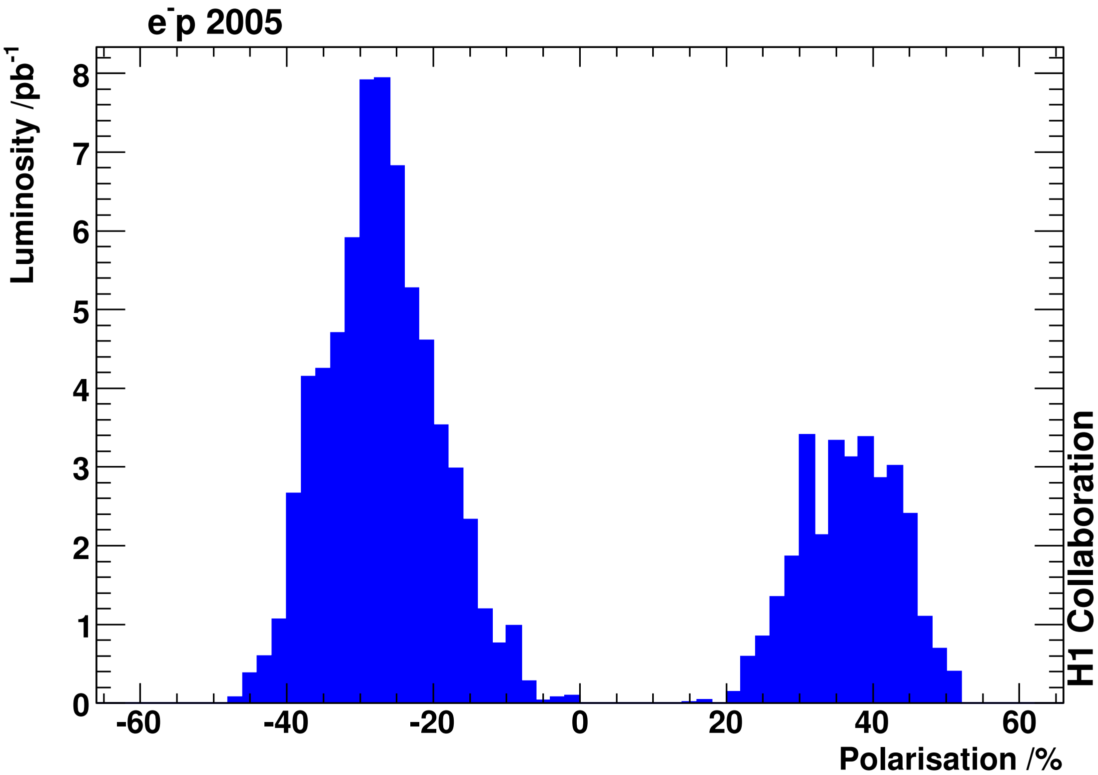

Figure 1: The polarisation profile weighted by the luminosity values for the e^-p data. The $L(R)$ sample corresponds to distribution having negative (positive) polarisation values.

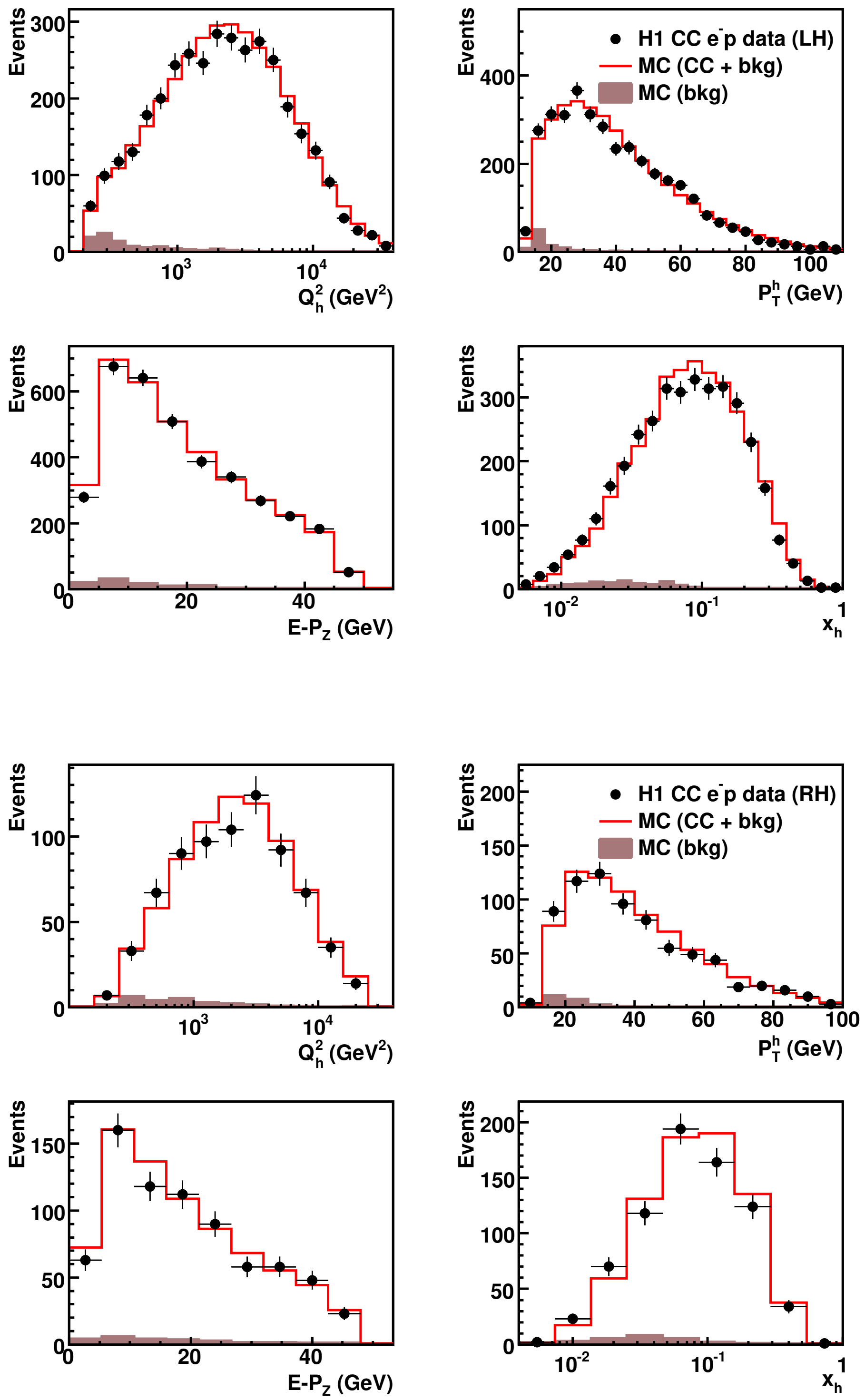

Figure 2: Distributions of Q_h^2, $P_{T,h}$, $E_h - p_{z,h}$ and x_h shown in upper and lower plots for the selected events in the left handed (LH) and right handed (RH) data sets. The Monte Carlo (MC) contributions from the charged current (CC) process and the ep background (bkg) processes are shown as open histograms with the latter contribution alone being shown as shaded histograms.

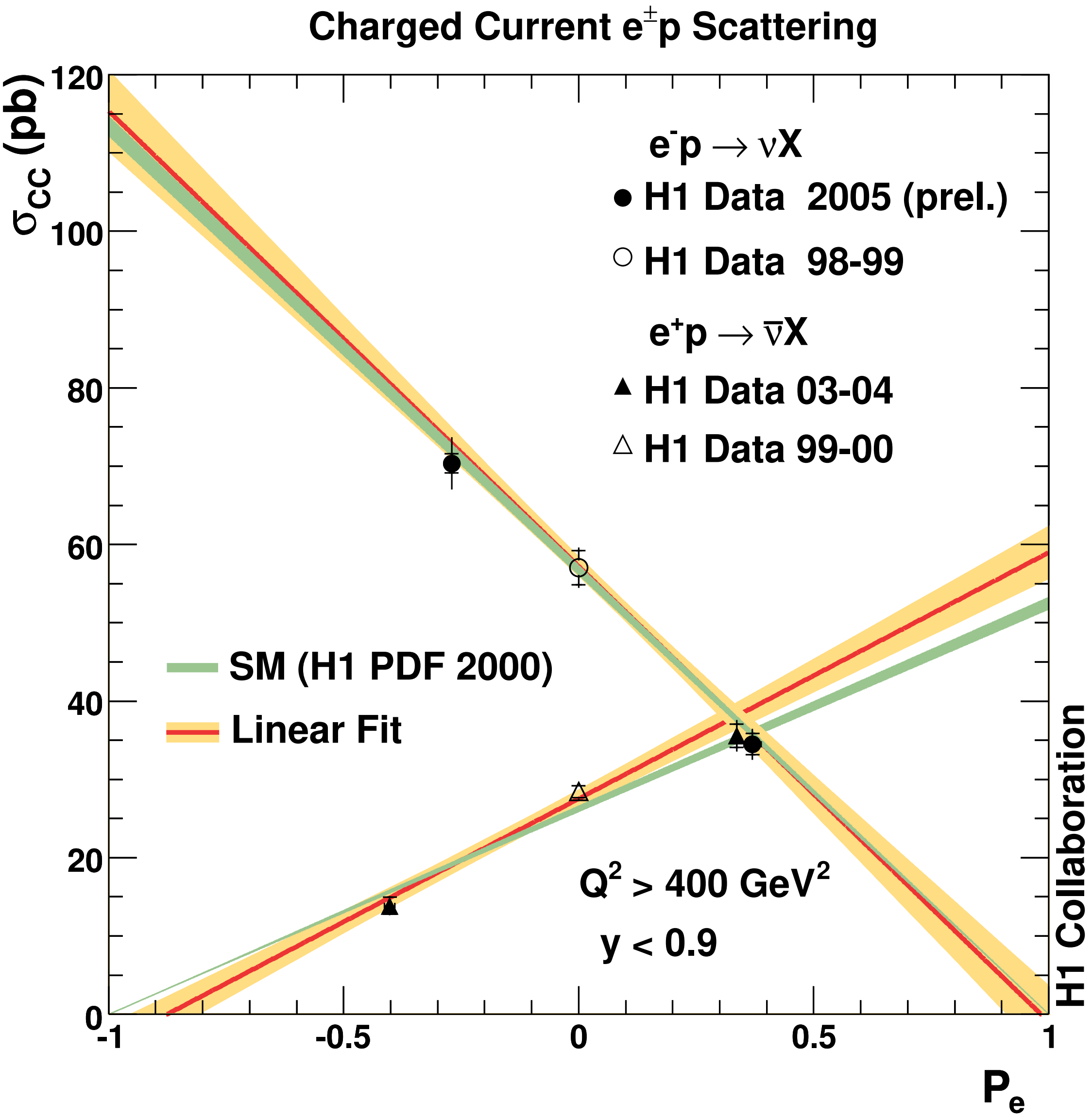

Figure 3: The dependence of the $e^{\pm}p$ CC cross section on the lepton beam polarisation P_e. The inner and outer error bars represent respectively the statistical and total errors. The uncertainties on the polarisation measurement are smaller than the symbol size. The data are compared to the Standard Model prediction based on the H1 PDF 2000 parametrisation (dark shaded band). The light shaded band corresponds to the resulting one-sigma contour of a linear fit to the data shown as the central line.

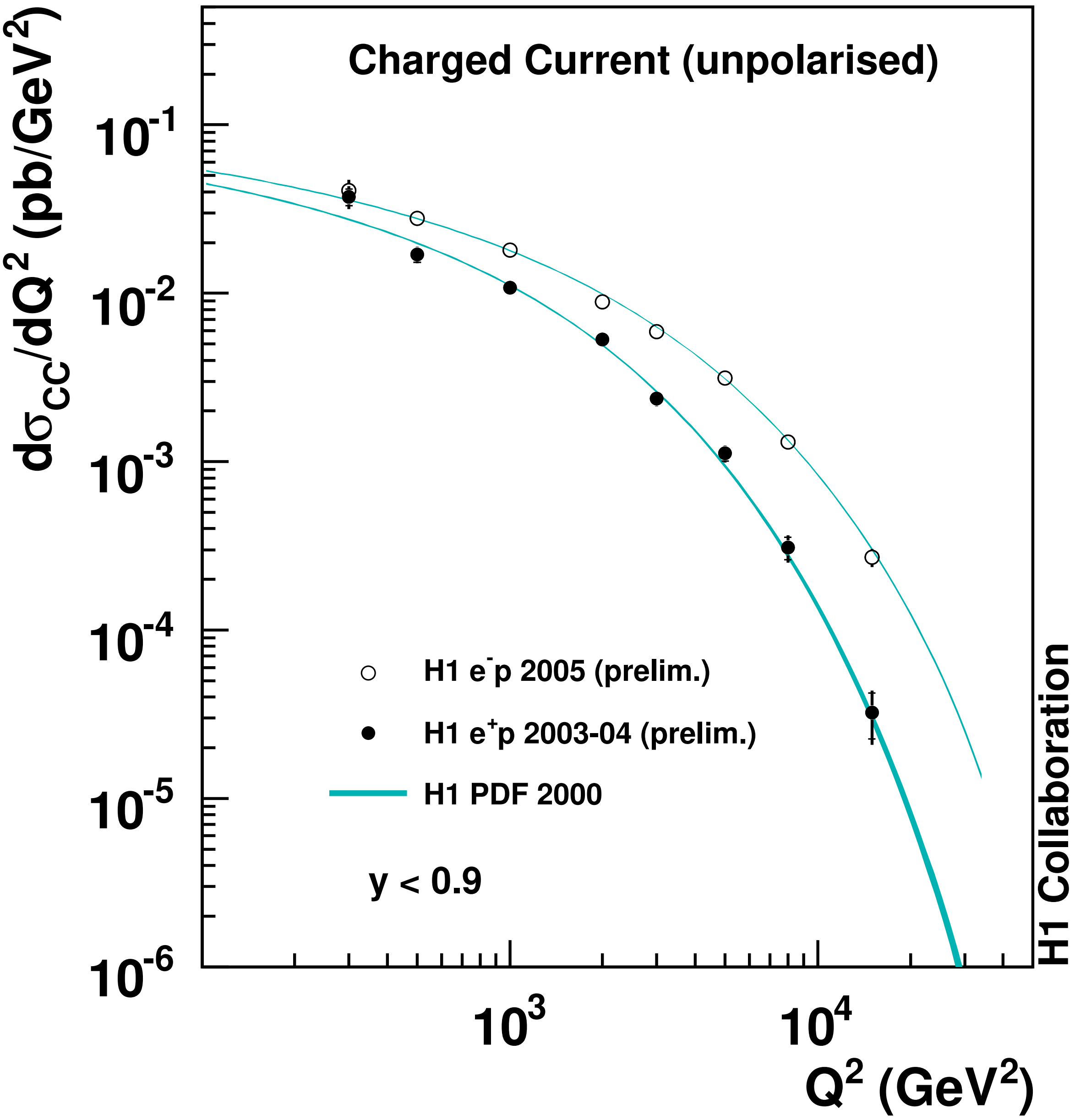

Figure 4: The Q^2 dependences of the CC cross sections $d\sigma/dQ^2$, shown for the e^-p (open points) and e^+p (solid points) data. The results are compared with the corresponding Standard Model expectations determined from the H1 PDF 2000 fit. The inner and outer error bars represent respectively the statistical and total errors.